TITLE: The Zero-Corrected, Gravity-Model Multiplier (ZERO-G): A novel method to estimate disease dynamics at the community-scale from passive surveillance data

Michelle V Evans[1]*, Felana A Ihantamalala[2,3], Mauricianot Randriamihaja[1,2], Andritiana Tsirinomen'ny Aina[2], Matthew H Bonds[2,3], Karen E Finnegan[2,3], Rado JL Rakotonanahary[2,3], Mbolatiana Raza-Fanomezanjanahary[2], Bénédicte Razafinjato[2], Oméga Raobela[4], Sahondraritera Herimamy Raholiarimanana[4], Tiana Harimisa Randrianavalona[4], Andres Garchitorena[1,2]

1. MIVEGEC, Univ. Montpellier, CNRS, IRD, Montpellier, France
2. NGO Pivot, Ranomafana, Ifanadiana, Madagascar
3. Department of Global Health and Social Medicine, Blavatnik Institute at Harvard Medical School, Boston, MA, USA
4. National Malaria Program, Ministry of Health, Antananarivo, Madagascar

* Corresponding Author: mv.evans.phd@gmail.com

ABSTRACT

Data on population health are vital to evidence-based decision making by public health officials, but are rarely adequately localized, particularly in rural areas where barriers to healthcare can result in extremely low ascertainment of cases by the health system. Here, we demonstrate a new method to estimate disease incidence at the community level from passive surveillance data collected at primary health centers. The zero-corrected, gravity-based multiplier (ZERO-G) method explicitly models sampling intensity as a function of health facility characteristics and statistically accounts for extremely low rates of ascertainment, resulting in an unbiased, standardized estimate of disease incidence at a spatial resolution nearly ten times finer than typically reported by the facility-based passive surveillance system. We assessed the robustness of this method by applying it to a case study of malaria incidence in a rural health district in southeastern Madagascar. ZERO-G decreased geographic and financial bias in the dataset by over 64% and doubled the agreement rate between spatial patterns in malaria incidence and prevalence rates. ZERO-G can be applied to other infectious diseases and settings, increasing the availability of long-term, high quality surveillance datasets at the community scale.

Key words: health care access; geographic bias; floating catchment area; malaria; Madagascar

INTRODUCTION

Health metrics are vital to public health efforts, allowing decision makers to better understand the state of population health and evaluate the impact of health interventions (Murray et al. 2004, Tatem et al. 2012). Many of these metrics are based on routine passive disease surveillance from facility-based health management information systems (HMIS), which record the number of disease cases received at each facility at a regular frequency. Health records are then aggregated, digitized, and transferred to the district, and eventually national, health offices (Amouzou et al. 2021). While the exact structure differs by country, each scale of spatial aggregation of the data in an HMIS corresponds to a specific level of the health system and corresponding health infrastructure. For example, national-level data are used by international organizations to monitor long-term, multi-country trends and inform policy; regional- and district-level surveillance data may be used by national public health offices to allocate resources within the country; and individual health facility information is used by district health offices for program management.

Missing from most HMIS are routine surveillance data at the scale of individual communities or villages. These data are needed for spatially targeted interventions for disease control in collaboration with community health programs, which primarily serve rural communities and play an integral role in achieving universal health coverage (World Health Organization et al. 2007, Rifkin 2018). While rural primary care facilities typically serve over ten thousand people spread along hundreds of square kilometers, community health workers serve between several hundred to a few thousand and their catchment is generally no bigger than 10 km^2. Due to geographic barriers in particular, systemic lack of access to health facilities for large portions of the population has resulted in community health becoming a central pillar of national health strategies globally (Perry 2020). The lack of long-term surveillance datasets at the community level impedes our ability to monitor changes in disease burdens over time, locally target or evaluate the impact of community-health interventions, create surveillance and forecasting systems at these levels, and generally incorporate health data into decision-making processes. Given the increasing role of community programs in providing primary health care and supporting disease control efforts, the lack of routine surveillance data at this level must be remedied.

There are several barriers to the creation of a routine surveillance system at the community level. First, community health workers often only diagnose and treat common illnesses for children under 5 years old (Young et al. 2012). Therefore, case notifications collected by community health workers are incomplete because they represent a small subset of

the population. Second, community health programs tend to be poorly funded, supported, and integrated within the larger health system (Kok et al. 2015, Hodgins et al. 2021), with negative consequences for data completeness and quality. For example, a case study in Malawi found that over 40% of community health reports contained errors when aggregation was conducted by CHWs due to lack of training and time available for reporting (Admon et al. 2013). Third, the existing structure of health system reporting often means that paper reports from the community level are submitted to district officials and integrated into the electronic HMIS system with significant delays, which limits their use for disease surveillance. An alternative is the use of health facility data disaggregated at the community level, which is becoming increasingly available with the development of new technologies such as eHealth systems. As these technologies become more common, the availability of data will become less of a barrier, but even when data remain disaggregated, there are issues of completeness and geographic bias due to heterogeneous access to care (Afrane et al. 2013, Ohrt et al. 2015, Garchitorena et al. 2021). These problems are exacerbated at fine spatial scales. For example, communities in rural areas with low access to care may be missed by routine health facility systems (Noor et al. 2003), significantly under-estimating disease burdens in these already vulnerable communities. Given the current lack of high-quality data at the community level, methods are needed to account for biases in data while retaining their spatial disaggregation.

At the scale of the government health district and higher, several methods have been developed to address these issues, particularly under-ascertainment of cases (Table 1). However, none of these adjustment methods result in estimates of disease incidence that are available at the spatial scale of individual communities and at a temporal regularity high enough to allow for rapid responses to epidemics. Existing methods are limited primarily by the frequency and spatial resolution of external data sources, such as large-scale surveys of disease prevalence or health-seeking behaviors. For example, information on healthcare utilization rates, such as that collected via Demographic and Health Surveys, is often collected nationally at the level of the district or region, and is inappropriate for use within smaller administrative zones. Prevalence surveys offer only a snapshot of malaria burden in time, and their inferences, while available at finer spatial scales, often only apply to annual estimates. In general, both forms of survey data are resource-intensive to obtain and are rarely available at spatial or temporal scales relevant to community health programs (Cibulskis et al. 2011). There is a need to leverage the spatial and temporal scale of passive surveillance data while adjusting for under-ascertainment biases in case reports, resulting in long-term, high-quality data on disease incidence at resolutions relevant to community health programs.

Table 1. Comparing the ZERO-G method to available methods for adjusting passive surveillance data.

Method	Temporal Scale	Spatial Scale	Data Required
Standard indirect estimators (e.g. WHO Malaria Report)	Annual	National	Estimates of health-seeking behavior, such as from DHS surveys
Prevalence-based geostatistical models (e.g. Malaria Atlas Project)	Annual	5x5 km	Prevalence survey, environmental variables
ZERO-G multiplier	Monthly or weekly, depending on frequency of data collection	Community or village level	Consultation data, geographic location of health system and population

Here, we introduce the zero-corrected, floating catchment gravity model multiplier (ZERO-G). This method accounts for under-ascertainment of cases by public health facilities, resulting in a long-term dataset of disease incidence at the scale of individual communities or villages. The method builds on work by Hyde et al. (Hyde et al. 2021) and combines an indirect estimation method with a floating catchment area model of healthcare access based on gravity models. The method first calculates a sampling intensity multiplier derived from consultation rates using a floating catchment area model (Delamater et al. 2019), and then scales disease incidence by this multiplier to adjust for spatio-temporal heterogeneity in access to healthcare. Importantly, this method relies solely on data available to local stakeholders: all-cause consultation rates, the focal disease incidence, and health facility characteristics. We demonstrate the method using a case-study of malaria passive surveillance in a rural health district in southeastern Madagascar. Then, we validate the method by comparing the estimated sampling intensity and malaria incidence rates to health-care seeking behavior and malaria prevalence from a district-representative cohort.

THE ZERO-G MULTIPLIER METHOD

The ZERO-G multiplier is an indirect estimation method that adjusts case data for known biases in case ascertainment to create high-quality monthly case notification data for multiple communities. Indirect estimation methods estimate the “true” rate of disease incidence or

prevalence from case data with low or uneven ascertainment rates by including information on the sampling intensity (e.g. healthcare use) in each administrative region (Hickman and Taylor 2005). ZERO-G specifically uses a benchmark multiplier method, which combines information on the number of cases recorded by the health system with information on the proportion of cases that are expected to be observed. In addition, it includes imputation methods for adjusting for extremely low ascertainment rates that result in zero cases reported. The final result is an estimation of disease incidence equal to the expected incidence if access to healthcare was identical across space and time.

ZERO-G consists of the following steps (Fig. 1):

1. Estimate sampling intensity using a floating catchment area model
2. Correct for low ascertainment rates that resulted in zero cases via spatio-temporal imputation methods
3. Identify optimum scaling factor for sampling intensity
4. Apply sampling intensity (multiplier) to zero-adjusted data (benchmark) via benchmark multiplier method

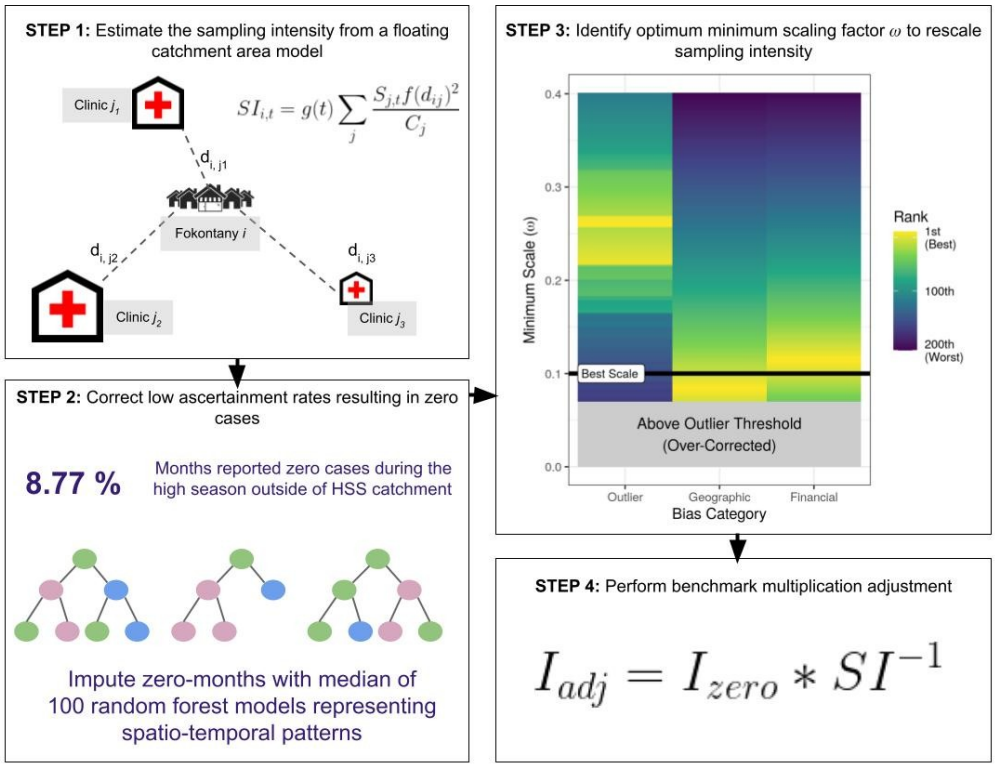

Figure 1. Workflow for adjusting incidence data using the floating catchment, zero-corrected multiplier (ZERO-G) method.

Step 1. Estimate sampling intensity via a floating catchment area model

Sampling intensity (SI) serves as the multiplier in a benchmark multiplier method, and can be derived from additional data sources (e.g. proportion in treatment, reported health-seeking behaviors, mortality rates). Often, these data are collected via surveys of healthcare seeking behavior and not available at a temporal or spatial scale that matches the case notification data. ZERO-G overcomes this by estimating a SI for each community for each month. In this method, SI is proportional to the probability that a disease case in that community and month is reported to the health system. It is estimated via a temporally-explicit floating catchment area (FCA) model, an established technique used to estimate spatial access to healthcare and health facility catchments (Luo and Qi 2009). Based on a gravity model, FCA models consider both the quantity and spatial accessibility of services at a health center for a given population by weighting the distance to care by the availability of services provided at each health center. Access to care in each community is then modeled as an "attractive force" to each health center and total access to care is the sum of these forces for a given community (Fig. 1, Step 1).

We used the modified two-step floating catchment area formulation of this metric, which allows for sub-optimal allocation of health resources via the inclusion of distance-weighted competition for each healthcare clinic's resources (Delamater 2013). We define the sampling intensity for each community *i* and month *t* ($SI_{i,t}$) following Equation 1:

$$SI_{i,t} = g(t) \sum_{j} \frac{S_{j,t} f(d_{ij})^2}{C_j} \qquad \text{Eq. 1}$$

This represents the sum of all healthcare services provided by each health center *j* at time *t* ($S_{j,t}$, Eq. 2), mediated by distance between each community *i* and the health center *j*, d_{ij}, and competition for services at each health center *j* by the total population across all communities (C_j, Eq. 4). Temporal trends in healthcare access are described by g(t), with the exact function dependent on temporal trends in healthcare access in the region being considered. For example, seasonal changes in health system use could be represented by a sinusoidal function.

Services provided by each health center *j* represent the "mass" of a gravity model, defined by Equation 2:

$$S_j = \sum_m \beta_m v_m \qquad \text{Eq. 2}$$

Each health center's mass (S_j) is equal to the sum of characteristics relevant to health services (v_m), weighted by a unique coefficient β_m. These characteristics will vary by health system, but should generally describe the quantity and quality of services available at the health center. They can be continuous variables (e.g. number of staff, number of beds) or binary variables (e.g. presence of a surgery unit, type of health center (hospital vs. clinic)). These services can vary over time, resulting in a different value for each month, allowing for changes in healthcare access following changes to the health system (e.g. opening or closing of clinics, new payment policies, change in staff numbers).

The effect of distance on spatial access to health center services is described by a distance-decay function $f(d_{ij})$. While the shape of this function may differ by the local context, distance-decay is most often described by an exponential function (Khan 1992) and is the recommended default when using this method (Eq. 3).

$$f(d_{ij}) = e^{-\lambda d_{ij}} \qquad \text{Eq. 3}$$

Competition for services at each health center *j* is defined as the sum of the population-weighted distance between all administrative zones and the health center, including a scaling factor β_c:

$$C_j = \beta_c \sum_k P_{k,t} f(d_{kj}) \qquad \text{Eq. 4}$$

The calculation of the SI includes several parameters that can be pre-specified (if known) or estimated by fitting the FCA model to all-cause consultation data with the focal disease removed (see Table S1 for description of parameters and ranges of values in the case study). Any model fitting method can be applied, such as maximum likelihood or Bayesian approaches. The recommended approach is to estimate the number of consultations for each community and month as a random variable with a binomial distribution with probability equal to the SI and size *n* equal to the population size of the community, although other distributions are possible.

Step 2. Correct for low ascertainment rates that resulted in zero cases via spatio-temporal imputation methods

In many instances, extremely low ascertainment rates combined with small populations in small geographic areas can result in zero reported cases for a month for a community. Because the benchmark multiplier is a scaling process, these values would remain unchanged (i.e. report zero incidence that month) after applying the benchmark multiplier step. The second step of ZERO-G is therefore replacing a subset of these extreme low incidence months (zero-incidence months) that are believed to be due to low ascertainment rates with new values using spatio-temporal imputation that incorporates seasonal and spatial patterns in incidence. Exactly which values should be replaced is context specific, and should take into account the seasonality of the focal disease and known spatial patterns in access to health care. For example, in the case study described below, only those zero-incidence months that occurred during the peak of the malaria season and in communities outside the catchment of a health-system strengthening initiative were replaced. Those that occurred outside of the malaria season or in the zone where health access is known to be higher were assumed to be representative of true spatio-temporal trends in incidence and were unchanged. Imputation is performed via 100 boosted regression tree models that estimate monthly incidence as a function of each community's identity, longitude, and latitude and the specific month of the zero-incidence occurrence, using the median of 100 imputations as the final imputed value. Imputed values are therefore a function of both spatial and temporal trends in the incidence data.

Step 3. Identify optimal minimum scaling factor for sampling intensity

The benchmark multiplier step of ZERO-G requires a SI multiplier greater than 0 and less than or equal to 1. A multiplier near zero results in a large change to the estimated incidence and a multiplier of one results in no change. SI is therefore linearly rescaled to fall between a minimum value (ω) and 1. For those communities that are considered representative of optimal healthcare access, the SI can be assigned a value of 1, meaning the incidence in these populations will be unchanged by the benchmark multiplier. All other communities will be standardized to equal the sampling intensity in these "high access" communities. The remaining SI values can then be rescaled between ω and 1. At a minimum, the optimal value of ω is that which most reduces the effect of geographic bias in the adjusted incidence rates. In addition to geographic biases, other factors can also be included to identify the optimal ω. In the case study below, we include financial bias and a limit on upper outliers in incidence rates in our selection of ω.

Step 4. Apply sampling intensity (multiplier) to zero-adjusted data (benchmark) via benchmark multiplier method

The rescaled sampling intensity (SI) and zero-corrected incidence data (I_{zero}) are then combined via the benchmark multiplier method to result in an adjusted estimate of monthly incidence (I_{adj}) for each community (Eq. 5):

$$I_{adj} = I_{zero} * SI^{-1} \qquad \text{Eq. 5}$$

In this equation, the zero-corrected incidence data serves as the benchmark while the inverse of the sampling intensity is the multiplier. Both are calculated to retain the temporal frequency and spatial resolution of the original dataset, meaning they have been estimated for each community and each time period. Retaining the frequency of the original dataset allows ZERO-G to account for temporal changes in ascertainment biases, such as seasonality or clinic closures, that may act differently across each community.

CASE STUDY: MALARIA INCIDENCE IN IFANADIANA, MADAGASCAR

We applied ZERO-G to malaria incidence in Ifanadiana District, Madagascar to demonstrate its utility in regions with highly heterogeneous rates of under-ascertainment. Ifanadiana is a district in the Vatovavy region of southeastern Madagascar. It has an estimated population of 183,000 people spread across 195 fokontany (smallest administrative unit comprising about 1000 people) within 15 communes. Each commune contains one primary health center level 2 (PHC2), and six of the larger communes also contain a primary health center level 1 (PHC1), which provides more basic care, for a total of 21 PHCs within the district. Beginning in 2014, the Madagascar Ministry of Public Health (MMoPH) and the non-governmental organization Pivot began a partnership to strengthen the health system, establishing Ifanadiana as a model health district. This intervention works across all levels of the health system, from community health at the household level to tertiary care at the regional hospital. At the level of the PHCs, the intervention includes renovation of PHC facilities, removal of point-of-care user fees, and joint recruitment of staff between Pivot and the MMoPH. As of January 2023, PHC-level interventions have been installed at 15 PHC2 across all 15 communes, and will be expanded to all levels of PHCs by the end 2023.

The primary barriers to healthcare at PHCs in Ifanadiana are geographical and financial. The majority of the district is rural and the transportation network is primarily non-motorized; over 70% of the population lives further than an hour travel time from a PHC (Ihantamalala et al. 2020). As such, geographical access to care at PHCs is highly unequal, and exhibits a strong

distance-decay relationship from PHC locations (Garchitorena et al. 2021). The second barrier is financial costs at the level of the individual. Nationally, nearly half of the total public health expenditure in Madagascar is borne by the individual (World Health Organization 2022), and these user fees are the most cited barrier to healthcare seeking across the district (Garchitorena et al. 2017). As such, we aimed to reduce the impact of geographic and financial bias in malaria incidence rates by adjusting the data using ZERO-G.

Data Collection

Monthly consultation data were collected at each PHC for the district of Ifanadiana from January 2016 to December 2021. Photos were taken of handwritten registries at each PHC, and patients' residences were manually geolocated to the precision of the fokontany. The number of all-cause consultations were reported by fokontany, as well as the number of malaria cases, as confirmed by rapid detection test. Because patient ages were provided in these registries, we were able to divide the number of consultations and malaria cases into three age groups for analysis: children under 5 years old, juveniles aged 5-14, and adults aged 15 and over. Ifanadiana suffers from stockouts of diagnostic materials, specifically rapid-detection tests (RDTs) (Cordier et al. 2020), leading to unconfirmed cases of malaria. We accounted for this reduced diagnostic capacity by scaling the confirmed malaria cases by the proportion of feverish patients who were tested via an RDT at each PHC during each month (n = 536). Information on the characteristics of each clinic by month was provided by Pivot's Monitoring and Evaluation for Research and Learning team.

Population data came from two sources. For the 80 fokontany that receive community health program support from Pivot, we used population estimates from a Pivot-led census conducted in 2021. For the remaining 115 fokontany, population estimates came from a national census conducted in 2018 by the Madagascar National Institute of Statistics. By interpolating population values between the 2018 census and the previous 1993 census, we estimated an average annual population growth rate of 2.0%. We applied this population growth rate to both datasets to obtain each fokontany's population by year. For both datasets, we assumed 18% of the population to be under 5 years old, 28.6% of the population to be aged 5 - 14 and the remainder to be 15 years old or above, based on the average age structure of the 80 fokontany that were censused in 2021.

Distances between residential areas and PHCs were calculated on a high-resolution transport network created via crowd-sourced mapping through a collaboration with Humanitarian OpenStreetMap. Over 20,000 km of footpaths and 100,000 buildings within the

district were mapped through a two-step validation process (Ihantamalala et al. 2020), resulting in an open-source dataset on OpenStreetMap. Using this dataset, we estimated the distance between each household and each PHC within the district, and aggregated this to the scale of the fokontany to result in an average distance to each PHC for each fokontany. Three fokontany lacked accurate routing information and so were excluded from the analysis.

We evaluated our estimates of the SI and adjusted malaria incidence rates using external data from a longitudinal cohort survey conducted in the district of Ifanadiana (IHOPE cohort). The IHOPE cohort has conducted population-representative surveys approximately every two years from 2014-2021 using a two-stage cluster sampling scheme involving 80 spatial clusters, each containing 20 households (Miller et al. 2018). We include data from 2016, 2018, and 2021 in this analysis. The IHOPE cohort is based on the internationally validated Demographic and Health Surveys and is implemented by the Madagascar National Institute of Statistics. See Miller et al. (2018) for further details on participant recruitment and study design. As part of the survey questionnaire, participants were asked if they were ill in the past four weeks and, if so, if they sought care at a public PHC. This data represented self-reported health-care seeking behavior, comparable to our estimates of sampling intensity. Malaria prevalence data was collected via rapid detection tests conducted as part of the IHOPE survey in 2021. Briefly, children under 15 years old who consented to the study were tested for active malaria infection using SD One Step Malaria HRP-II(P.f) and pLDH(Pan) Antigen Rapid Tests. Those who tested positive were provided with a standard treatment of artesunate amodiaquine and paracetamol, with duration and dosage in accordance with national guidelines. In total, this resulted in 3774 samples across 80 clusters and 109 fokontany.

Applying the ZERO-G multiplier

Estimating Sampling Intensity

We estimated the sampling intensity for each fokontany and month combination in our dataset following the methods described above for each age class (children, juveniles, and adults) using non-malarial consultations at health centers. We included five traits of the health center in our calculation of S_i:

1. whether the PHC fell within the initial Pivot service catchment,
2. if point-of-care user fees (consultation costs and medications) had been removed,
3. the number of staff at the PHC during each month,
4. level of health clinic (PHC1 or PHC2, with PHC2 providing more services),

5. distance from the PHC to the District office, which provides supplies, medications, and supervision.

In addition, two new PHC2 were opened in the district during the study period, one in Ampasinambo in November 2016 and one in Ambiabe in April 2018, which we accounted for in our calculation of SI. Notably, ZERO-G allows for health center traits that change over time, which we used to include monthly staffing changes and user fee removal interventions that were implemented over the study period.

We included linear and seasonal adjustments to the SI via the g(t) function (Eq. 6), to account for increasing access to healthcare over time and seasonality in major diseases in Madagascar (i.e. respiratory disease, diarrheal disease). It includes a linear coefficient (β_t) and a sine-function, to account for seasonality, parameterized by ϕ.

$$g(t) = e^{\beta_1 t + \beta_2 \frac{sin(2\pi(t+\phi)/12)+1}{2}} \qquad \text{Eq. 6}$$

We used an exponential function to describe the distance-decay relationship, allowing the shape of this relationship to vary between fokontany within the Pivot catchment and those outside of the Pivot catchment by applying a scaling coefficient (β_s). To reduce computational time, we set a maximum limit on the distance between a community and the PHC (d_{ij}) at 25 km, slightly above the maximum distance of a fokontany to the nearest PHC in Ifanadiana (22.1 km).

Finally, we estimated the number of non-malarial consultations *y* as a random variable with a binomial distribution with the probability equal to the SI and size *n* equal to the population size of the fokontany. A total of 11 parameters were estimated via maximum-likelihood estimation (MLE) (Table S1). Some fokontany had extremely low consultation rates and reported zero consultations for over 50% of the study period. We excluded these fokontany (n = 43) from the model fitting exercise, but did estimate their SI from the fit model. We used a two-step MLE estimation process. First, we performed a grid search via a latin hypercube sample of 1,000 samples of coarse parameter space to identify the ten parameter sets with the lowest negative log-likelihood. We then performed a second MLE using the BFGS algorithm via the optim function in the *stats* package in R (R Core Team 2021), using the parameters from the ten parameter sets with the lowest negative log-likelihood from the first step as the starting parameters. We assessed each of these ten iterations for convergence and selected the parameter set with the lowest negative log-likelihood as the optimal fit. From the optimal parameter set, we estimated an SI for each fokontany-month combination via Eq. 1.

Zero-correcting via boosted regression tree imputations

Thirty-seven fokontany reported zero malaria cases during at least half of the study period, totaling 3468 (28.4%) of fokontany-month samples. We chose to only replace zeros in those fokontany that were outside of Pivot's initial catchment (n = 140), assuming ascertainment was high enough in fokontany in Pivot's initial catchment that zeros were due primarily to seasonal trends in incidence and not under-ascertainment. We also only replaced zeros that occurred during the malaria season (November through May), assuming zeros outside of this season were representative of the low incidence characteristic of that time period. This resulted in 8.57 to 9.06% of fokontany-month incidence values being imputed for each age class, an average of 7.65 months per fokontany (range: 0-25), for those fokontany outside of Pivot's initial catchment. These values were imputed 100 times using boosted regression trees that estimated new monthly incidence as a function of each foktonany's identity, longitude and latitude and the specific month of the study period using the *mice* package(Buuren and Groothuis-Oudshoorn 2011). The final imputed value was the median of 100 imputations.

Identifying the optimal scaling factor (ω) and applying the benchmark multiplier

We manually set SI to 1 for those fokontany which had an average annual consultation rate over 1 consultation per capita-year, defined as "high access fokontany" (n = 19). We then explored a range of minimum values of the scaling factor, from 0.002 to 0.4 with a resolution of 0.002. We identified the minimum value that met requirements with regards to upper incidence outliers, geographic bias, and financial bias (Fig. 1):

1. Upper incidence outliers: A very low ω could result in incidence rates that are unrealistically high. To limit the overcorrection of incidence rates, we limited ω to values that resulted in a proportion of upper incidence outliers less than 3x the proportion of upper incidence outliers seen in the high access fokontany in the full dataset. An upper incidence outlier was defined as an annual incidence rate above the mean annual incidence rate + 3 *sd* in the high access fokontany.
2. Geographic bias: We calculated geographic bias by estimating the Spearman's ranked correlation coefficient between the distance to the nearest PHC and the mean adjusted annual incidence for each fokontany. A correlation coefficient of zero corresponded to no bias. We calculated this bias for each potential value of ω, and ranked each value by how well it corrected the bias.
3. Financial bias: We calculated financial bias as the mean ratio of annual incidence rates in fokontany with user fee reimbursement to incidence in fokontany not benefiting from

user fee reimbursement. A ratio of 1 corresponded to no bias. We calculated this bias for each potential value of ω, and ranked each value by how well it corrected the bias.

We calculated these three metrics (proportion of upper incidence outliers, geographic bias, and financial bias) for the full range of minimum values of the scaling factor (ω) and ranked the minimum scale factors by their performance for each metric, with lower ranks corresponding to the least bias. To identify the optimum value of ω, we first identified the subset of ω that met our upper incidence outlier criteria described above. Then, we identified the value of ω that resulted in the lowest mean rank of correction for geographic and financial bias while minimizing the difference in performance between the two, measured via the coefficient of variation.

The SI was rescaled between ω and 1 and then used in combination with the zero adjusted data from step 3 to perform benchmark multiplication (Eq. 4). This resulted in a final dataset of monthly malaria incidence for each age class from January 2016 - June 2021 for 192 fokontany, adjusted so that the sampling intensity was standardized for all fokontany and matched that found in the “high access” fokontany.

Evaluating Adjusted Datasets

We evaluated our estimates of the SI and adjusted malaria incidence rates using external data from the IHOPE cohort. Self-reported healthcare seeking behavior was paired spatially to SI estimates by assigning a value to a fokontany if a village from the cluster was in that fokontany and was paired temporally by taking the average of the SI during the 6 month period containing the months when the IHOPE survey was conducted in each year (January through June for 2016 and 2021 and July through December for 2018), to reduce the impact of month outliers in consultation rates on SI estimates. We assessed the agreement between the two datasets by calculating the correlation between estimated SI and the proportion of residents reporting illness who attended PHCs using Clifford’s modified t-test, which controls for spatial autocorrelation (Clifford et al. 1989). We assessed the correlation separately for each year (2016, 2018, 2021), including 109 fokontany per year.

We evaluated the ability of our adjusted incidence rates to accurately represent malaria burdens by comparing adjusted incidence rates to malaria prevalence data collected via the IHOPE cohort in 2021. The two datasets were paired spatially by assigning a value to a fokontany if a village from the cluster was in that fokontany and was paired overtime by matching the month of the IHOPE survey to the month of the incidence rates. We compared adjusted incidence rates for children under 15 years old to prevalence rates of children under 15 years old from the IHOPE cohort for all fokontany with information in both datasets (n= 109) via

Clifford's modified t-test. We also assessed the ability of the adjusted incidence data to correctly identify hot spots of malaria, defined as the quartile of fokontany with the highest prevalence values.

Ethics Statement

Use of aggregate monthly consultation counts from PHCs in Ifanadiana District for this study was authorized by the Medical Inspector of Ifanadiana. The IHOPE longitudinal survey implemented informed consent procedures approved by the Madagascar National Ethics Committee and the Madagascar Institute of Statistics. Household-level de-identified data from the IHOPE survey were provided to the authors for the current study. We recognize that all research is conducted within the surrounding socio-political context and risks reproducing existing inequalities within the research team and across research partners. We've chosen to explicitly reflect on power dynamics and equitable authorship within the context of this research project in an accompanying reflexivity statement (Supplemental Materials).

RESULTS

Estimating the Sampling Intensity

We estimated the SI by fitting a floating catchment area model to non-malaria consultation data from January 2016 - December 2021. The resulting model performed well at reproducing the non-malaria consultation data (under-5: Spearman's $\rho = 0.615$, p-value<0.001; juvenile: Spearman's $\rho = 0.609$, p-value<0.001; adult: Spearman's $\rho = 0.704$, p-value<0.001). When averaged over all fokontany per month, it accurately represented the temporal trends in the non-malaria consultation data (under-5: Spearman's $\rho = 0.389$, p-value <0.002; juvenile: Spearman's $\rho = 0.608$, p-value <0.001; adult: Spearman's $\rho = 0.629$, p-value <0.001). When averaged across time to result in one average SI per fokontany, it also was able to capture spatial and fokontany-specific differences in consultation rates and model predictions closely matched the non-malaria consultation rates (under-5: Spearman's $\rho =0.819$, p-value <0.001; juvenile: Spearman's $\rho =0.800$, p-value <0.001; adult: Spearman's $\rho =0.840$, p-value <0.001).

The spatial patterns in the estimated SI mirrored spatial patterns in self-reported healthcare seeking behavior from the IHOPE longitudinal survey (Fig. 2). The estimated SI and self-reported healthcare seeking rates were significantly correlated across all years (Clifford's t-test; 2016: $\rho = 0.54$ (p=0.002), 2018: $\rho = 0.67$ (p = 0.008), 2021: $\rho = 0.59$ (p = 0.01)). Both data sources estimate higher healthcare access at fokontany nearer the national transportation network, specifically the paved road that runs east-west through the district, and in close

proximity to PHCs. In addition, the two datasets were in agreement that the majority of the district has low access to healthcare.

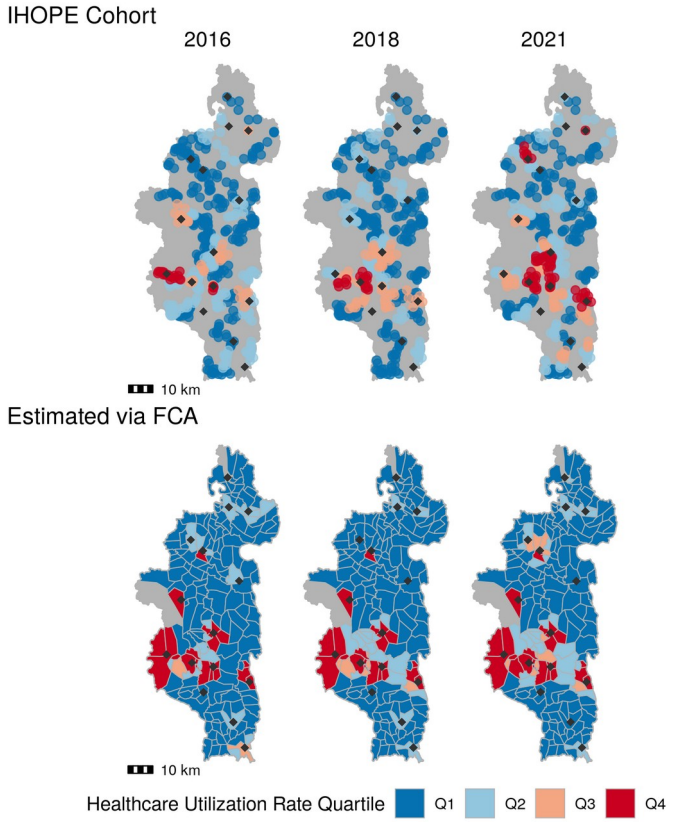

Figure 2. The sampling intensity estimated via the floating catchment area (FCA) method (bottom row) closely approximates self-reported healthcare seeking rates from the IHOPE cohort (top row). Shading represents rates grouped into quartiles, with Q1 corresponding to the lowest healthcare utilization rate and Q4 to the highest. Diamond points show the location of level-2 PHCs. Top row: Cluster-level healthcare seeking rates are illustrated for each village in a cluster across the three survey years. Bottom row: The scaled sampling intensity estimated via a floating-catchment area method.

Reduction of Bias in Malaria Incidence due to Geographic and Financial Barriers to Care

We selected a minimum SI scale value (ω) that best corrected geographic bias and bias due to cost-of-care reimbursement policies (Fig. 1, Fig. 3). The unadjusted dataset showed evidence of geographic bias; average annual incidence of malaria in children under-5 in a fokontany was negatively correlated with the distance from that fokontany to the nearest PHC (Spearman's ρ = -0.617, p-value < 0.001, Fig. 3A), showing an exponential distance decay. The adjusted dataset, by comparison, demonstrated a much weaker, though still significant, negative relationship between average annual incidence and distance to the nearest PHC (Spearman's ρ = -0.222, p-value<0.01, Fig. 3A). Fokontany whose populations attended PHCs where user fees were

reimbursed reported 2.48 times higher incidence than those that did not benefit from the reimbursement policy in the unadjusted dataset (Fig. 3B). Applying the ZERO-G method drastically reduced this bias; the average annual incidence in these fokontany was 1.01 times the incidence in fokontany with cost-of-care-reimbursement (Fig. 3B).

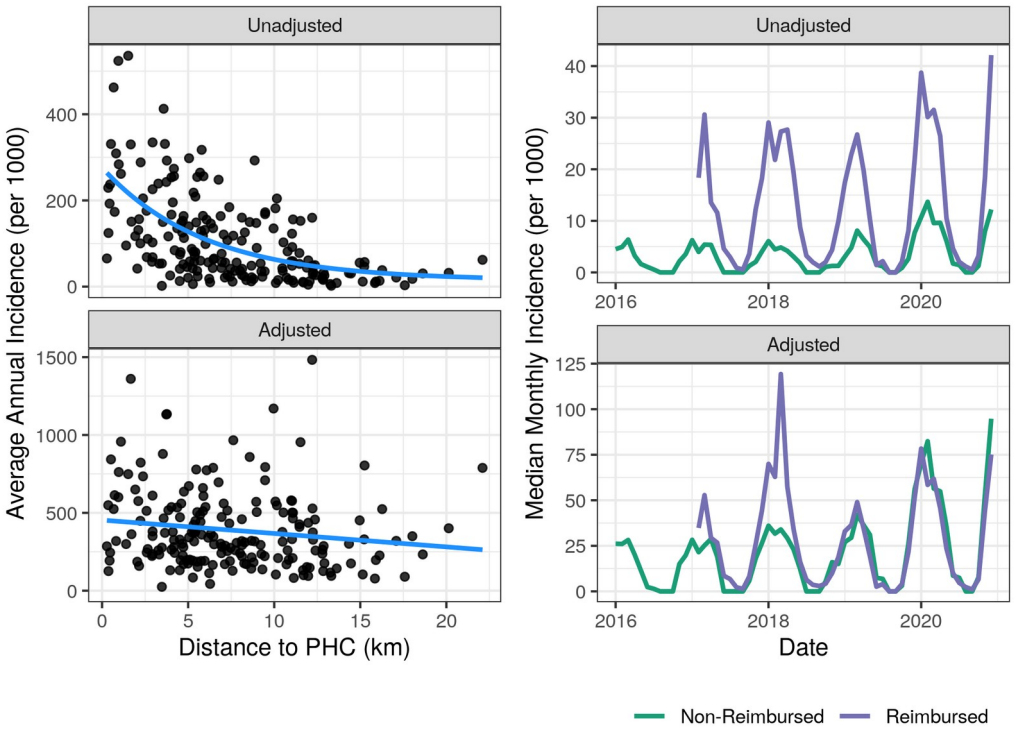

Figure 3. The ZERO-G adjustment method greatly reduces geographical and financial bias in malaria incidence rates. Left: Each point represents the average annual malaria incidence rates for a fokontany over the period of 2016-2020, with the x-axis showing the distance to the nearest PHC. The smoothed line is the exponential (unadjusted) or linear (adjusted) fit between average annual incidence and distance to PHC. Right: The median monthly malaria incidence rates across fokontany whose closest PHC does or does not offer fee reimbursement. Fee reimbursement began in January 2017.

Comparing Unadjusted and Adjusted Datasets

Comparing the unadjusted and adjusted datasets, we estimated that unadjusted case notifications are capturing on average 32.4% of symptomatic malaria cases in the district. This differed by year, with the lowest percentage of 29.2% in 2020 and the highest of 49.6% in 2017. The level of under-ascertainment also varied across fokontany. On average, the adjusted annual incidence in a fokontany was 9.82 (range: 1- 1533) times the unadjusted annual incidence rate. However, when this was calculated omitting fokontany and year combinations

that reported zero malaria cases in a year (26 out of 944), this ratio was reduced to 6.59 (range: 1 - 113).

Validation with Prevalence Data

We validated ZERO-G by comparing incidence rates and prevalence rates in children under 15 years old. Unadjusted incidence rates were negatively correlated with RDT positivity rates (Spearman's ρ = -18.2, p-value = 0.06) and showed no evidence of a correlation with the proportion of symptomatic and RDT positive individuals (Spearman's ρ = -0.04, p-value = 0.6). After adjusting the data, we found a positive correlation between incidence and prevalence rates (Spearman's ρ = 0.2031, p-value = 0.04). While the estimated correlation coefficient between incidence rates and the proportion of symptomatic and RDT positive children was positive in the adjusted dataset, it remained insignificant (Spearman's ρ = 0.127, p-value = 0.2). The adjusted dataset also doubled the number of correctly-ranked fokontany into quantiles that matched those from the prevalence data (Fig. 4). The adjusted dataset correctly ranked 38 of 104 fokontany, compared to 19 in the unadjusted dataset.

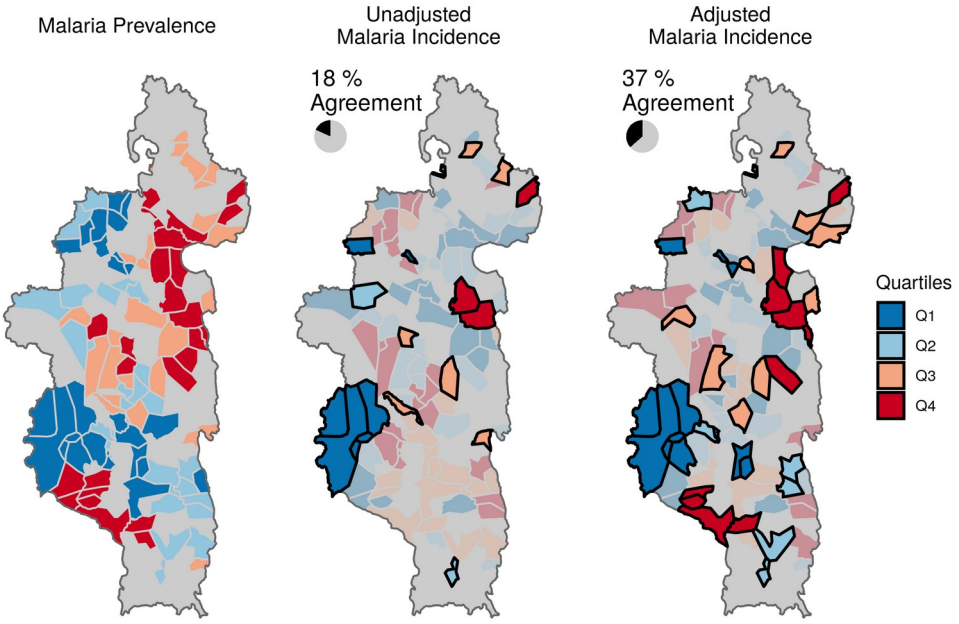

Figure 4. The adjustment method results in monthly malaria incidence rates in 2021 that more closely correspond to measures of malaria prevalence in children under 15 years old. Left: Malaria prevalence as measured by rapid-detection tests (RDT) in children under 15 years old from the IHOPE cohort survey. Colors represent quartiles from Q1 (lowest incidence) to Q4 (highest incidence). Middle: Monthly malaria incidence in the unadjusted dataset. Quartiles that match those in the prevalence data are highlighted in black. Right: Monthly malaria incidence in the adjusted data. Quartiles that match those in the prevalence data are

highlighted in black. Monthly incidence has been chosen to correspond to the month in which the IHOPE survey was conducted for that fokontany.

DISCUSSION

There is a critical need for routine surveillance systems to produce estimates at the spatial scale of individual communities so that control interventions can be targeted in collaboration with community health programs. However, HMIS data are rarely kept disaggregated at this scale and, when they are, they suffer from under-estimation of incidence that varies across space and time, preventing their use at these scales. We developed an adjustment method called the ZERO-G multiplier that combines a gravity-model of healthcare access with a benchmark multiplier method to create long-term routine surveillance data at the community-scale adjusted for under-ascertainment due to uneven health care access. We demonstrated this method by applying it to malaria case notification data from 192 communities and over 5 years of surveillance in a rural District of Madagascar. This method reduced geographical and financial bias in malaria incidence rates by 64% and 99%, respectively. In addition, we validated this method with two external, population-representative datasets and found strong agreement with self-reported healthcare access and malaria prevalence rates. Through this method, we were able to obtain estimates that approximate long-term active surveillance data at fine-spatial scales using only passive surveillance data, suggesting that the passive surveillance system only reported about a third of all symptomatic malaria cases.

ZERO-G greatly reduced bias in malaria incidence rates in passive surveillance data in our study setting. In Ifanadiana district, per capita health system utilization rates are twice as high for fokontany within 5km of a health center than those further away (Garchitorena et al. 2021), and we found similar trends in the unadjusted malaria data (Fig. 3). Geographic bias in the malaria data was therefore primarily reduced by accounting for low sampling intensity at those fokontany further than 5 km from a PHC (Fig. 2). Financial costs represent a significant barrier to healthcare seeking, particularly for low-income communities, and differential user fee reimbursement policies over time (e.g. implementation of universal health coverage) can result in healthcare access patterns changing as a function of this (James et al. 2005, Yates 2009). In Ifanadiana, the removal of user fees via reimbursement policies in part of the district led to a sudden and sustained 65% increase in utilization rates (Garchitorena et al. 2017). ZERO-G removed this bias, resulting in similar incidence rates regardless of when and where reimbursement policies were in place. ZERO-G also resulted in data that more accurately identified malaria prevalence hotspots and coldspots than the unadjusted data, performing twice as well as the unadjusted data. However, the adjusted dataset only correctly categorized 37% of

fokontany into ranked quantiles, illustrating the difficulty in matching incidence data to prevalence data. The relationship between malaria prevalence and incidence is non-linear, particularly for adults (Cameron et al. 2015), which can complicate matched ranking of prevalence and incidence.

Unlike other methods, which rely on external datasets describing sampling intensity that are collected at coarse spatial resolutions and infrequently (e.g. DHS, MICS, or other survey data), ZERO-G uses data that match the spatial and temporal resolution of the case notification data. This allows it to retain the original spatial and temporal scales at which the data was collected while relying solely on public health and demographic data that is easily accessible to public health actors. Population data can be sourced at fine-scale administrative levels via national census data or via open-source datasets such as PopGrid (Leyk et al. 2019). Information on PHC locations and services are collected by Ministries of Health or available via regional, open-source datasets (e.g. Maina et al. 2019). We used a field-verified transport network created via OpenStreetMap to estimate the distance between a population and a PHC, which accurately represents patients' distance to PHCs (Ihantamalala et al. 2020); however, these transportation networks are not globally available. When transportation networks are not available, open-source databases of populations' distances to PHCs and other services could serve as suitable substitutes (e.g. Nelson et al. 2019, Weiss et al. 2020). Finally, consultation rates are commonly tracked by health systems and are increasingly recorded via electronic health management information systems (Kumar et al. 2018, Siyam et al. 2021), facilitating their use in these estimates.

ZERO-G differs from existing adjustment methods in several ways. First, it uses monthly estimates of sampling intensity in the indirect estimate step rather than data from annual or inter-annual population surveys. Most adjustment methods do not account for changes in healthcare seeking behavior due to seasonality or temporal shifts to the health system (e.g. changes in PHC staffing rates), and are therefore limited to inference at an annual frequency (Gibbons et al. 2014). Second, the resulting dataset is available at the same spatial scale at which it is collected, rather than spatially interpolated between points or aggregated to coarser resolutions. We build on work by Hyde et al. (2021), which proposed a similar indirect estimation adjustment method for malaria data that featured a monthly frequency at the fokontany scale, but dealt with extreme low incidence values by spatially smoothing estimates between neighboring fokontany, introducing spatial structure into the adjusted dataset and removing existing natural variation. In addition, ZERO-G explicitly models the sampling intensity as a function of geographic and health-system characteristics in all the facilities surrounding a

community via a gravity model instead of using information from the closest facility in a linear model, as in Hyde et al. (Hyde et al. 2021). Because of this, changes in the health system can be directly incorporated into calculations of sampling intensity in near real-time. It also allows for estimation of sampling intensity in unsampled communities or months through these modeled processes, rather than relying on interpolation.

There are several limitations that should be taken into consideration when evaluating or implementing ZERO-G. First, active surveillance of malaria in our study area is limited, and we only had access to one study of malaria prevalence at a spatial-scale finer than 5 x 5 km. Therefore, we were only able to assess our method's ability to reproduce spatial patterns in malaria burden, and not temporal patterns. However, our model results agree with national-level trends in malaria, which witnessed over a 40% increase in confirmed malaria cases in 2020 (World Health Organization 2021), suggesting we are capturing temporal trends as well. Second, we introduced a further source of uncertainty via the imputation of zero-incidence samples due to extremely low ascertainment. This replaced months during the malaria season reporting zero cases with predictions from a spatio-temporal model, mirroring established methods (Gething et al. 2006), and replaced a small fraction of the overall data (8.77%). Finally, our method does not include a step to disaggregate consultation rates to a finer spatial scale than that reported by the PHC, often a major limiting step to accessing disease incidence data at a fine spatial scale. In Ifanadiana, the standard reporting system aggregates consultations at the level of the health facility catchment. We manually digitized health registers to obtain community-level data, a time- and resource-intensive process. However, the increased availability of electronic systems at the level of primary and community health care represents an opportunity to apply this method directly and in real time to data at fine spatial scales.

In conclusion, ZERO-G represents a promising new method for adjusting passive surveillance data for under-ascertainment bias in regions with low and heterogeneous healthcare seeking rates, developed specifically for use at the community level. This method can serve as part of a wider toolkit of statistical techniques used to improve targeted health system responses. In a case study in a rural health district in Madagascar, it was able to reduce geographic and financial bias in malaria incidence and the resulting dataset more closely approximated spatial trends in malaria prevalence. ZERO-G can be applied to any case notification dataset that suffers from geographic bias due to case under-ascertainment, including both infectious and non-communicable diseases. It is particularly suited to rural areas, where geographic isolation strongly influences healthcare access (Weiss et al. 2020). As spatially-explicit health metrics become an increasingly important tool for precision public health

interventions, there is an urgent need to obtain and use quality data sources at the community scale. Statistical methods such as ZERO-G can be an important tool to support the role of community health programs in the local targeting of interventions for disease control.

DATA AVAILABILITY STATEMENT

All code and data needed to reproduce this study are available in a figshare repository (doi: 10.6084/m9.figshare.22154492).

ACKNOWLEDGMENTS

We would like to thank the health professionals who collect passive surveillance data in addition to serving their patients and the Pivot data collection team for their work collecting and digitizing this data. We would also like to thank the staff at Pivot who supervise much of this work, particularly Laura Cordier. We would also like to thank Ann Miller and Marius Randriamanambintsoa for their support of the IHOPE longitudinal survey.

FUNDING STATEMENT

This work was supported by internal funding from Pivot (https://www.pivotworks.org/), which provided salary for FAI, MR, ATA, MHB, KEF, RJLR, M R-F, and BR. It was also supported by a grant from the Agence Nationale de la Recherche (Project ANR-19-CE36-0001-01), granted to AG, which supported AG, MR, and MVE. The funders had no role in study design, data collection and analysis, decision to publish, or preparation of the manuscript.

REFERENCES

Admon, A. J., J. Bazile, H. Makungwa, M. A. Chingoli, L. R. Hirschhorn, M. Peckarsky, J. Rigodon, M. Herce, F. Chingoli, P. N. Malani, and B. L. Hedt-Gauthier. 2013. Assessing and improving data quality from community health workers: a successful intervention in Neno, Malawi. Public Health Action 3:56–59.

Afrane, Y. A., G. Zhou, A. K. Githeko, and G. Yan. 2013. Utility of Health Facility-based Malaria Data for Malaria Surveillance. PLOS ONE 8:e54305.

Amouzou, A., C. Faye, K. Wyss, and T. Boerma. 2021. Strengthening routine health information systems for analysis and data use: a tipping point. BMC Health Services Research 21:618.

Buuren, S. van, and K. Groothuis-Oudshoorn. 2011. mice: Multivariate Imputation by Chained Equations in R. Journal of Statistical Software 45:1–67.

Cameron, E., K. E. Battle, S. Bhatt, D. J. Weiss, D. Bisanzio, B. Mappin, U. Dalrymple, S. I. Hay, D. L. Smith, J. T. Griffin, E. A. Wenger, P. A. Eckhoff, T. A. Smith, M. A. Penny, and P. W. Gething. 2015. Defining the relationship between infection prevalence and clinical incidence of Plasmodium falciparum malaria. Nature Communications 6:8170.

Cibulskis, R. E., M. Aregawi, R. Williams, M. Otten, and C. Dye. 2011. Worldwide Incidence of Malaria in 2009: Estimates, Time Trends, and a Critique of Methods. PLOS Medicine 8:e1001142.

Clifford, P., S. Richardson, and D. Hemon. 1989. Assessing the Significance of the Correlation between Two Spatial Processes. Biometrics 45:123–134.

Cordier, L. F., K. Kalaris, R. J. L. Rakotonanahary, L. Rakotonirina, J. Haruna, A. Mayfield, L. Marovavy, M. G. McCarty, A. Tsirinomen’ny Aina, B. Ratsimbazafy, B. Razafinjato, T. Loyd, F. Ihantamalala, A. Garchitorena, M. H. Bonds, and K. E. Finnegan. 2020. Networks of Care in Rural Madagascar for Achieving Universal Health Coverage in Ifanadiana District. Health Systems & Reform 6:e1841437.

Delamater, P. L. 2013. Spatial accessibility in suboptimally configured health care systems: A

modified two-step floating catchment area (M2SFCA) metric. Health & Place 24:30–43.

Delamater, P. L., A. M. Shortridge, and R. C. Kilcoyne. 2019. Using floating catchment area (FCA) metrics to predict health care utilization patterns. BMC Health Services Research 19:144.

Garchitorena, A., F. A. Ihantamalala, C. Révillion, L. F. Cordier, M. Randriamihaja, B. Razafinjato, F. H. Rafenoarivamalala, K. E. Finnegan, J. C. Andrianirinarison, J. Rakotonirina, V. Herbreteau, and M. H. Bonds. 2021. Geographic barriers to achieving universal health coverage: evidence from rural Madagascar. Health Policy and Planning 36:1659–1670.

Garchitorena, A., A. C. Miller, L. F. Cordier, R. Ramananjato, V. R. Rabeza, M. Murray, A. Cripps, L. Hall, P. Farmer, M. Rich, A. V. Orlan, A. Rabemampionona, G. Rakotozafy, D. Randriantsimaniry, D. Gikic, and M. H. Bonds. 2017. In Madagascar, Use Of Health Care Services Increased When Fees Were Removed: Lessons For Universal Health Coverage. Health Affairs 36:1443–1451.

Gething, P. W., A. M. Noor, P. W. Gikandi, E. A. A. Ogara, S. I. Hay, M. S. Nixon, R. W. Snow, and P. M. Atkinson. 2006. Improving Imperfect Data from Health Management Information Systems in Africa Using Space–Time Geostatistics. PLOS Medicine 3:e271.

Gibbons, C. L., M.-J. J. Mangen, D. Plass, A. H. Havelaar, R. J. Brooke, P. Kramarz, K. L. Peterson, A. L. Stuurman, A. Cassini, E. M. Fèvre, and M. E. Kretzschmar. 2014. Measuring underreporting and under-ascertainment in infectious disease datasets: a comparison of methods. BMC Public Health 14:147.

Hickman, M., and C. Taylor. 2005. Indirect Methods to Estimate Prevalence. Pages 113–131 *in* Z. Sloboda, editor. Epidemiology of Drug Abuse. Springer-Verlag, New York.

Hodgins, S., M. Kok, D. Musoke, S. Lewin, L. Crigler, K. LeBan, and H. B. Perry. 2021. Community health workers at the dawn of a new era: 1. Introduction: tensions confronting large-scale CHW programmes. Health Research Policy and Systems 19:109.

Hyde, E., M. H. Bonds, F. A. Ihantamalala, A. C. Miller, L. F. Cordier, B. Razafinjato, H.

Andriambolamanana, M. Randriamanambintsoa, M. Barry, J. C. Andrianirinarison, M. N. Andriamananjara, and A. Garchitorena. 2021. Estimating the local spatio-temporal distribution of malaria from routine health information systems in areas of low health care access and reporting. International Journal of Health Geographics 20:8.

Ihantamalala, F. A., V. Herbreteau, C. Révillion, M. Randriamihaja, J. Commins, T. Andréambeloson, F. H. Rafenoarimalala, A. Randrianambinina, L. F. Cordier, M. H. Bonds, and A. Garchitorena. 2020. Improving geographical accessibility modeling for operational use by local health actors. International Journal of Health Geographics 19:27.

James, C., S. S. Morris, R. Keith, and A. Taylor. 2005. Impact on child mortality of removing user fees: simulation model. BMJ 331:747–749.

Khan, A. A. 1992. An integrated approach to measuring potential spatial access to health care services. Socio-Economic Planning Sciences 26:275–287.

Kok, M. C., S. S. Kane, O. Tulloch, H. Ormel, S. Theobald, M. Dieleman, M. Taegtmeyer, J. E. Broerse, and K. A. de Koning. 2015. How does context influence performance of community health workers in low- and middle-income countries? Evidence from the literature. Health Research Policy and Systems 13:13.

Kumar, M., D. Gotz, T. Nutley, and J. B. Smith. 2018. Research gaps in routine health information system design barriers to data quality and use in low- and middle-income countries: A literature review. The International Journal of Health Planning and Management 33:e1–e9.

Leyk, S., A. E. Gaughan, S. B. Adamo, A. de Sherbinin, D. Balk, S. Freire, A. Rose, F. R. Stevens, B. Blankespoor, C. Frye, J. Comenetz, A. Sorichetta, K. MacManus, L. Pistolesi, M. Levy, A. J. Tatem, and M. Pesaresi. 2019. The spatial allocation of population: a review of large-scale gridded population data products and their fitness for use. Earth System Science Data 11:1385–1409.

Luo, W., and Y. Qi. 2009. An enhanced two-step floating catchment area (E2SFCA) method for measuring spatial accessibility to primary care physicians. Health & Place 15:1100–1107.

Maina, J., P. O. Ouma, P. M. Macharia, V. A. Alegana, B. Mitto, I. S. Fall, A. M. Noor, R. W. Snow, and E. A. Okiro. 2019. A spatial database of health facilities managed by the public health sector in sub Saharan Africa. Scientific Data 6:1–8.

Miller, A. C., A. Garchitorena, V. Rabeza, M. Randriamanambintsoa, H.-T. Rahaniraka Razanadrakato, L. Cordier, M. A. Ouenzar, M. B. Murray, D. R. Thomson, and M. H. Bonds. 2018. Cohort Profile: Ifanadiana Health Outcomes and Prosperity longitudinal Evaluation (IHOPE). International Journal of Epidemiology 47:1394–1395e.

Murray, C. J. L., A. D. Lopez, and S. Wibulpolprasert. 2004. Monitoring global health: time for new solutions. BMJ : British Medical Journal 329:1096–1100.

Nelson, A., D. J. Weiss, J. van Etten, A. Cattaneo, T. S. McMenomy, and J. Koo. 2019. A suite of global accessibility indicators. Scientific Data 6:266.

Noor, A. M., D. Zurovac, S. I. Hay, S. A. Ochola, and R. W. Snow. 2003. Defining equity in physical access to clinical services using geographical information systems as part of malaria planning and monitoring in Kenya. Tropical medicine & international health: TM & IH 8:917–926.

Ohrt, C., K. W. Roberts, H. J. W. Sturrock, J. Wegbreit, B. Y. Lee, and R. D. Gosling. 2015. Information Systems to Support Surveillance for Malaria Elimination. The American Journal of Tropical Medicine and Hygiene 93:145–152.

Perry, H. B., editor. 2020. Health for the people: National community health worker programs from Afghanistan to Zimbabwe. USAID MCHIP.

R Core Team. 2021. R: A language and environment for statistical computing. R Foundation for Statistical Computing, Vienna, Austria.

Rifkin, S. B. 2018. Alma Ata after 40 years: Primary Health Care and Health for All—from consensus to complexity. BMJ Global Health 3:e001188.

Siyam, A., P. Ir, D. York, J. Antwi, F. Amponsah, O. Rambique, C. Funzamo, A. Azeez, L. Mboera, C. J. Kumalija, S. F. Rumisha, I. Mremi, T. Boerma, and K. O'Neill. 2021. The burden of recording and reporting health data in primary health care facilities in five low- and

lower-middle income countries. BMC Health Services Research 21:691.

Tatem, A. J., S. Adamo, N. Bharti, C. R. Burgert, M. Castro, A. Dorelien, G. Fink, C. Linard, M. John, L. Montana, M. R. Montgomery, A. Nelson, A. M. Noor, D. Pindolia, G. Yetman, and D. Balk. 2012. Mapping populations at risk: improving spatial demographic data for infectious disease modeling and metric derivation. Population Health Metrics 10:8.

Weiss, D. J., A. Nelson, C. A. Vargas-Ruiz, K. Gligorić, S. Bavadekar, E. Gabrilovich, A. Bertozzi-Villa, J. Rozier, H. S. Gibson, T. Shekel, C. Kamath, A. Lieber, K. Schulman, Y. Shao, V. Qarkaxhija, A. K. Nandi, S. H. Keddie, S. Rumisha, P. Amratia, R. Arambepola, E. G. Chestnutt, J. J. Millar, T. L. Symons, E. Cameron, K. E. Battle, S. Bhatt, and P. W. Gething. 2020. Global maps of travel time to healthcare facilities. Nature Medicine 26:1835–1838.

World Health Organization. 2021. World malaria report 2021. World Health Organization, Geneva.

World Health Organization. 2022. Global Health Expenditure Database.

World Health Organization, PEPFAR, and UNAIDS. 2007. Task shifting : rational redistribution of tasks among health workforce teams : global recommendations and guidelines. World Health Organization.

Yates, R. 2009. Universal health care and the removal of user fees. The Lancet 373:2078–2081.

Young, M., C. Wolfheim, D. R. Marsh, and D. Hammamy. 2012. World Health Organization/United Nations Children's Fund Joint Statement on Integrated Community Case Management: An Equity-Focused Strategy to Improve Access to Essential Treatment Services for Children. The American Journal of Tropical Medicine and Hygiene 87:6–10.